J|A|C|S
ARTICLES
Published on Web 12/27/2005

Ultrafast Excited-State Dynamics in Vitamin B_{12} and Related Cob(III)alamins

Joseph J. Shiang,[†] Allwyn G. Cole,[†] Roseanne J. Sension,*[,†] Kun Hang,[‡] Yuxiang Weng,[‡] Jenna S. Trommel,[‡] Luigi G. Marzilli,*[,‡,§] and Tianquan Lian*[,‡]

Contribution from the Department of Chemistry and Department of Physics, University of Michigan, Ann Arbor, Michigan 48109-1055, and Department of Chemistry, Emory University, 1515 Pierce Drive, Atlanta, Ga 30322

Received July 1, 2005; E-mail: rsension@umich.edu; lmarzil@emory.edu; tlian@emory.edu

Abstract: Femtosecond transient IR and visible absorption spectroscopies have been employed to investigate the excited-state photophysics of vitamin B_{12} (cyanocobalamin, CNCbl) and the related cob(III)alamins, azidocobalamin (N_3Cbl), and aquocobalamin (H_2OCbl). Excitation of CNCbl, H_2OCbl, or N_3Cbl results in rapid formation of a short-lived excited state followed by ground-state recovery on time scales ranging from a few picoseconds to a few tens of picoseconds. The lifetime of the intermediate state is influenced by the σ-donating ability of the axial ligand, decreasing in the order CNCbl > N_3Cbl > H_2OCbl, and by the polarity of the solvent, decreasing with increasing solvent polarity. The peak of the excited-state visible absorption spectrum is shifted to ca. 490 nm, and the shape of the spectrum is characteristic of weak axial ligands, similar to those observed for cob(II)alamin, base-off cobalamins, or cobinamides. Transient IR spectra of the upper CN and N_3 ligands are red-shifted 20−30 cm^{-1} from the ground-state frequencies, consistent with a weakened Co−upper ligand bond. These results suggest that the transient intermediate state can be attributed to a corrin ring π to Co $3d_{z^2}$ ligand to metal charge transfer (LMCT) state. In this state bonds between the cobalt and the axial ligands are weakened and lengthened with respect to the corresponding ground states.

Introduction

Vitamin B_{12}, cyanocobalamin or CNCbl (see Figure 1), is an essential human nutrient, first discovered as the cure for pernicious anemia.[1] Two B_{12}-dependent enzymes, methylmalonyl-CoA mutase and methionine synthase, are essential human enzymes. These enzymes incorporate active alkylcobalamins derived from CNCbl. Methylcobalamin (MeCbl), or a closely related methylcorrinoid, functions as a methyl donor in methionine synthase and other methyltransferase enzymes. Methyltransferase enzymes function through heterolytic cleavage of the cobalt−carbon bond to form cob(I)alamin with the methyl group formally transferred as a methyl cation; thus, the cobalt cycles between Co(I) and Co(III) states.[2,3] In contrast, adenosylcobalamin-dependent (coenzyme B_{12}, AdoCbl) enzymes catalyze rearrangement reactions that proceed via mechanisms involving organic radicals generated by homolysis of the coenzyme cobalt−carbon bond to produce an adenosyl radical and cob(II)alamin.[3,4] Vitamin B_{12} is the stable form of cobalamin originally isolated from liver and is the form often packaged in multivitamins and nutritional supplements.

The absorption spectra of cobalamins are characteristic of both the oxidation state and the nature of the upper and lower axial ligands bound to the central cobalt.[5,6] The changes in the spectrum that accompany changes in oxidation state and ligation are illustrated in Figure 2. As a consequence, UV−visible absorption spectroscopy has often been used to identify changes in oxidation state and ligation of cobalamins and related species, and time-resolved UV−visible spectroscopy allows characterization of intermediate states in cobalamin systems. In previous papers we have reported the results of a series of transient absorption studies probing the photoinduced homolysis of alkylcobalamins, investigating dynamics on time scales ranging from femtoseconds to nanoseconds.[7−12] These studies have demonstrated that the photolysis mechanism is dependent on the nature of the alkyl ligand and the solvent environment of the alkylcobalamin.

[†] University of Michigan.
[‡] Emory University.
[§] Current address: Chemistry Department, Louisiana State University, Baton Rouge, LA, 70803.

(1) Dolphin, D., Ed. *B_{12}*; John Wiley and Sons: New York, 1982; Vol. 1.
(2) Banerjee, R.; Matthews, R. G. *FASEB J.* **1990**, *4*, 1450−1459.
(3) Ludwig, M. L.; Matthews, R. G. *Annu. Rev. Biochem.* **1997**, *66*, 269−313.
(4) Marsh, E. N. G. *Biochemistry* **1999**, *34*, 139−154.
(5) Giannotti, C. Electronic Spectra of B_{12} and Related Systems. In *B_{12}*; Dolphin, D., Ed.; John Wiley and Sons: New York, 1982; pp 393−430.
(6) Pratt, J. M. In *Chemistry and Biochemistry of B_{12}*; Banerjee, R., Ed.; Wiley: New York, 1999; pp 113−164.
(7) Walker, L. A., II; Jarrett, J. T.; Anderson, N. A.; Pullen, S. H.; Matthews, R. G.; Sension, R. J. *J. Am. Chem. Soc.* **1998**, *120*, 3597−3603.
(8) Walker, L. A., II; Shiang, J. J.; Anderson, N. A.; Pullen, S. H.; Sension, R. J. *J. Am. Chem. Soc.* **1998**, *120*, 7286−7292.
(9) Shiang, J. J.; Walker, L. A., II; Anderson, N. A.; Cole, A. G.; Sension, R. J. *J. Phys. Chem. B* **1999**, *103*, 10532−10539.
(10) Yoder, L. M.; Cole, A. G.; Walker, L. A., II; Sension, R. J. *J. Phys. Chem. B* **2001**, *105*, 12180−12188.
(11) Cole, A. G.; Yoder, L. M.; Shiang, J. J.; Anderson, N. A.; Walker, L. A., II; Banaszak Holl, M. M.; Sension, R. J. *J. Am. Chem. Soc.* **2002**, *124*, 434−441.

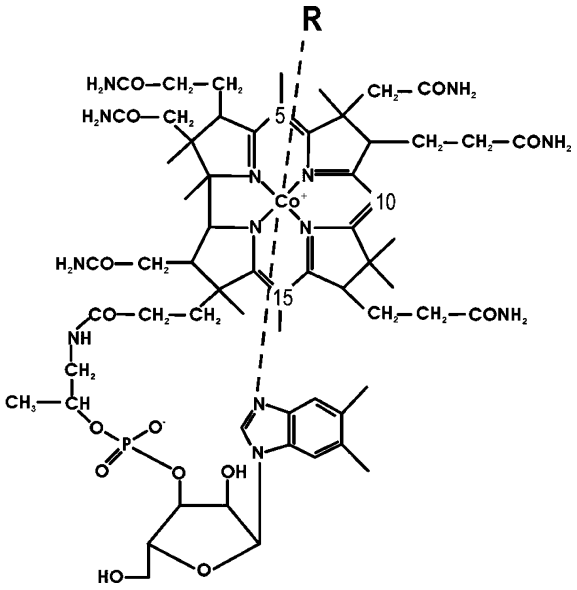

Figure 1. Schematic diagram of cobalamin. In vitamin B_{12} (CNCbl) the R group ligating the Co is a cyano (−C≡N) group; in the other compounds investigated here, it is an azido ($-N_3$) group or a water molecule. In the biologically active alkylcobalamins R is either a 5′-deoxyadenosyl group or a methyl group. The carbons labeled 5, 10, and 15 define the principal axes of the corrin ring. In-plane polarized electronic transitions of the corrin tend to be polarized along or nearly along the C15−C5 axis (long axis) or the Co−C10 axis (short axis).

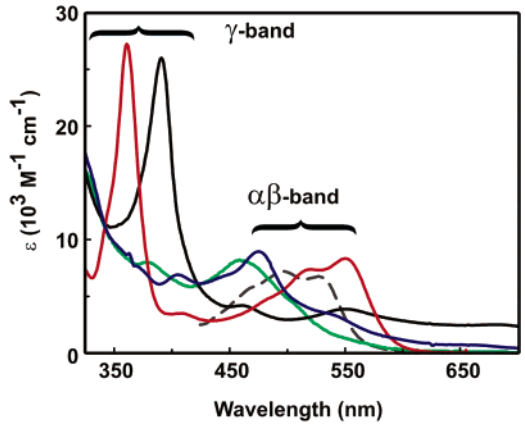

Figure 2. UV−visible absorption spectra of cob(I)alamin (black), cob(II)alamin (blue) and CNCbl (red), base-off AdoCbl at pH 2.5 (green) and cyanocobinamide (gray dashed, from ref 13). All of the spectra were obtained in water.

On the other hand, many non-alkylcobalamins, such as cyanocobalamin, azidocobalamin (N_3Cbl), and aquocobalamin (H_2OCbl), are believe to be photostable under visible light illumination, although it was reported that cyanocobalamin underwent photoaquation with a very small quantum yield ($\sim 10^{-4}$) in which upper ligand was replaced by water.[14] In the present contribution we describe the results of a transient absorption study probing the photochemistry or photophysics of CNCbl after 400 and 520 nm excitation and N_3Cbl and H_2OCbl after 400 nm excitation. The results presented here demonstrate that the cobalt−upper ligand bonds in these three cobalamins do not dissociate under conditions of single photon excitation at 400 or 520 nm. In each case a single transient excited state formed on a subpicosecond time scale was observed for each cobalamin. This state decays to ground state in 3−20 ps, depending on axial ligand and solvent. To facilitate the assignment of the excited state, we also measured the transient infrared spectra of CNCbl and N_3Cbl. These results are interpreted in the light of recent DFT calculations of the electronic structures CNCbl, H_2OCbl, and MeCbl.[15−20]

Experimental Section

Transient absorption measurements were performed using two different laser systems. The first system used a home-built self-mode-locked titanium:sapphire oscillator, running at 88 MHz and producing 20 fs, 2 nJ pulses. These pulses were amplified in a kHz regenerative amplifier. The resulting laser beam was centered at approximately 800 nm, providing 300 μJ, 60−80 fs pulses at 1 kHz repetition rate. The pump pulse was either the second harmonic of the laser at 400 nm, or a pulse centered at 520 nm, generated by sending the 800 nm laser pulse into a home-built noncollinear optical parametric amplifier (NOPA) constructed according to the design of Riedle and co-workers.[21] The probe pulse was generated by directing the undoubled fundamental remaining after the initial BBO crystal into a second piece of sapphire or into a flow cell containing ethylene glycol. The experimental setup for pump−probe measurements has been described earlier.[7−9] The pump and probe pulses were focused through a 100 μm pinhole to optimize pulse overlap. The entire continuum was used to measure the time-dependent difference spectrum as described previously.[7] For precise measurements of the time decay, interference filters were used to select the desired probe wavelengths. In one experiment the output of the NOPA was compressed to 28 fs using a prism pair. A beam splitter was used to generate pump and probe pulses at 520 nm. For all of these measurements the polarization of the pump and probe beams were set at the magic angle of 54.7° with respect to each other.

Pump−probe measurements on cobalamins were also made using a femtosecond tunable visible/IR laser system.[22,23] Briefly, the 800 nm output pulse of a regeneratively amplified femtosecond Ti:sapphire laser system from Clark-MXR (1 kHz, 100 fs, 0.9 mJ/pulse) was split into two beams to generate a 400-nm pump pulse and a visible or IR probe pulse. The visible probe pulses were obtained by focusing approximately 6 μJ of the 800 nm pulses into a 2-mm thick sapphire window to produce a white light continuum. Adjusting the intensity of the 800 -nm beam using an iris and neutral density filters optimized the stability of the continuum. Tunable probe pulses in the 430−650 nm region were selected with a variable interference filter with 10 nm bandwidth. The absorbance changes were measured as a function of delay time to obtain kinetics traces at wavelengths from 450 to 650 nm, with an interval of 5 to 10 nm. The probe pulses were split into the signal and reference beams, and detected by two matched photodiodes (PDA50). To obtain an overview of the global spectral change, transient difference spectra were constructed from the kinetics traces. To ensure that the absolute magnitudes of the absorbance change measured at different

(12) Sension, R. J.; Cole, A. G.; Harris, A. D.; Fox, C. C.; Woodbury, N. W.; Lin, S.; Marsh, E. N. G. *J. Am. Chem. Soc.* **2004**, *126*, 1598−1599.
(13) Hamza, M. S. A.; Pratt, J. M. *J. Chem. Soc., Dalton Trans*. **1994**, 1373−1376.
(14) Vogler, A.; Hirschmann, R.; Otto, H.; Kunkley, H. *Ber. Bunsen-Ges. Phys. Chem.* **1976**, *80*, 420−424.
(15) Andruniow, T.; Kozlowski, P. M.; Zgierski, M. Z. *J. Chem. Phys.* **2001**, *115*, 7522−7533.
(16) Stich, T. A.; Brooks, A. J.; Buan, N. R.; Brunold, T. C. *J. Am. Chem. Soc.* **2003**, *125*, 5897−5914.
(17) Brooks, A. J.; Vlasie, M.; Banerjee, R.; Brunold, T. C. *J. Am. Chem. Soc.* **2004**, *126*, 8167−8180.
(18) Ouyang, L.; Randaccio, L.; Rulis, P.; Kurmaev, E. Z.; Moewes, A.; Ching, W. Y. *J. Mol. Struct. (THEOCHEM)* **2003**, *622*, 221−227.
(19) Kurmaev, E. Z.; Moewes, A.; Ouyang, L.; Randaccio, L.; Rulis, P.; Ching, W. Y.; Bach, M.; Neumann, M. *Europhys. Lett.* **2003**, *62*, 582−587.
(20) Ouyang, L. Z.; Rulis, P.; Ching, W. Y.; Šlouf, M.; Nardin, G.; Randaccio, L. *Spectrochim. Acta Part A* **2005**, *61*, 1647−1652.
(21) Wilhelm, T.; Piel, J.; Riedle, E. *Opt. Lett.* **1997**, *22*, 1494−1496.
(22) Ghosh, H. N.; Asbury, J. B.; Lian, T. *J. Phys. Chem. B* **1998**, *102*, 6482.
(23) Wang, Y. Q.; Asbury, J. B.; Lian, T. *J. Phys. Chem. A* **2000**, *104*, 4291−4299.

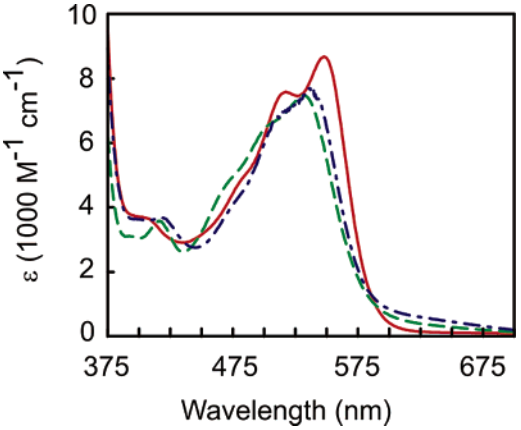

Figure 3. UV−visible spectra of CNCbl (red solid line), N_3Cbl (blue dot−dashed line), and H_2OCbl (green dashed line) dissolved in ethanol.

wavelengths can be reliably compared, the spatial overlap of pump probe beams was optimized and time zero was determined for each probe wavelength.

Tunable IR probe pulses from 3 to 10 μm were generated using optical parametric amplification in conjunction with difference frequency generation (DFG). A Clark IR Optical Parametric Amplifier was used to convert the 0.6 mJ/pulse at 800 nm into two tunable near-IR pulses from 1.1 to 2.5 μm, which were combined in a $AgGaS_2$ DFG crystal to generate the mid-IR probe pulse from 3 to 10 μm. About 60% of the IR probe pulse was used as a signal beam for measuring the absorption of sample and 40% of the IR probe pulse was used as a reference beam for normalizing the laser intensity fluctuation. After passing through an IR monochromator with a resolution of 2−3 cm^{-1}, the two beams were measured separately by two Mercury Cadmium Telluride (MCT) detectors. Alternatively, a 32-element MCT array detector was used to simultaneously collect 32 probe wavelengths. The zero delay time and instrument response were determined in a silicon wafer for the transient IR measurements.[22] Polarization of pump beam with respect to probe beam was set at magic angle (54.7°). The pump beam at the sample was about 500 μm, and the diameters of the IR and visible probe beams were about 300 and 200 μm, respectively.

Cyanocobalamin from Sigma was used without further purification. Aquocobalamin and azidocobalamin were synthesized according to a published procedure.[24] All solvents used were of reagent grade. The concentration of samples varied from 0.2 to 10 mM, limited by solubility, and no acid, base, or buffer was added. A UV−visible spectrum of CNCbl in water is shown in Figure 2. UV−visible spectra of CNCbl, N_3Cbl, and H_2OCbl in ethanol solutions are shown in Figure 3. The cobalamin solutions were flowed to prevent sample heating and the long-term build-up of photoproducts in the probed volume. Path lengths used varied from 150 to 750 μm in transient IR experiments and from 0.5 to 2 mm in transient visible experiments. UV−visible and IR spectra of samples showed no noticeable change after laser experiments.

Results

Visible Transient Absorption of Cyanocobalamin. Transient difference spectra obtained following the excitation of CNCbl in water and ethanol at 400 nm are shown in Figure 4. The transient difference spectra consist of a bleach of the ground-state absorption at around 550 nm and transient absorption bands around 480 and 600 nm. The data obtained in water exhibit surprisingly clear isosbestic points at 507 and 578 nm and demonstrate the clean decay of the excited-state back to the ground state. The difference spectra for CNCbl obtained in ethanol are similar to those obtained in water. Again, the overall shape of the difference spectrum does not change between 1 and 100 ps, as indicated by two clear isosbestic points located near 508 and 588 nm. The absorption and bleach features decay to baseline by 100 ps. Although the overall shape and magnitude of the difference spectra in water and ethanol are similar, the relative intensity of the red absorption wing is much stronger in water than in ethanol.

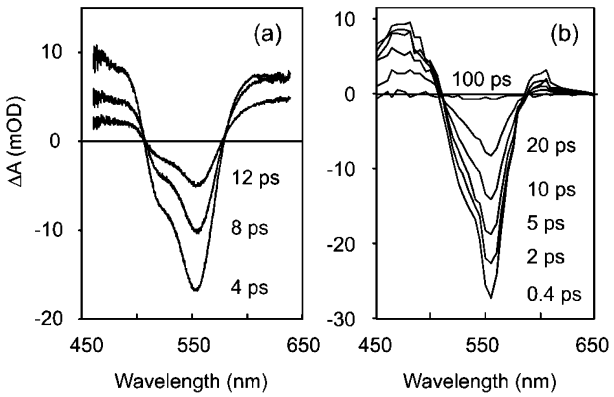

Figure 4. Visible transient difference spectra obtained following excitation of CNCbl at 400 nm (a) in water and (b) in ethanol.

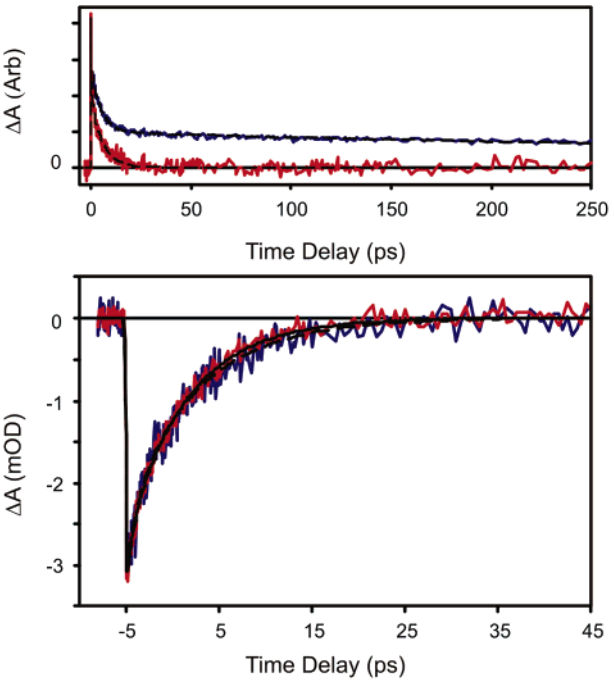

Figure 5. (Upper panel) Decay of the absorption observed at 600 nm following excitation of CNCbl in water at 400 nm. The red trace was obtained with a sub-μJ excitation pulse. The blue trace was obtained with a strong pump pulse ca. 30 times more intense than that used for the red trace. For ease of comparison the two traces have been scaled to the same peak intensity. The black lines represent fits of the data to a sum of two (red trace) or three (blue trace) exponential decay components. (Lower panel) Decay of the bleach monitored at the peak of the bleach (560 nm) following excitation at 400 nm (red) and 520 nm (blue). The solid and dashed black lines are fits of the data to a biexponential decay.

The evolution of the difference spectrum for CNCbl in H_2O, monitored at 560 nm, is shown in Figure 5. The signal at 560 nm is characterized by a 6.7 ± 0.8 ps decay to baseline and is independent of the excitation wavelength (520 or 400 nm). The same decay to baseline is observed at 600 nm. The data plotted

(24) Calafat, A. M.; Marzilli, L. G. *J. Am. Chem. Soc.* **1993**, *115*, 9182−9190.

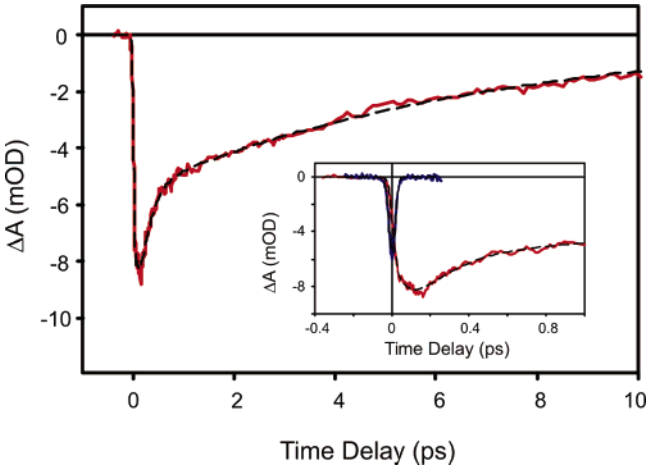

Figure 6. Decay of the bleach monitored at 520 nm following excitation of CNCbl at 520 nm. The solid line represents a fit of the data to an exponential rise followed by a biexponential decay. (Inset) Early time behavior. The blue line illustrates the instrument function, determined from an optical Kerr effect measurement. The instrument response function is well modeled by a Gaussian with a fwhm of 40 fs.

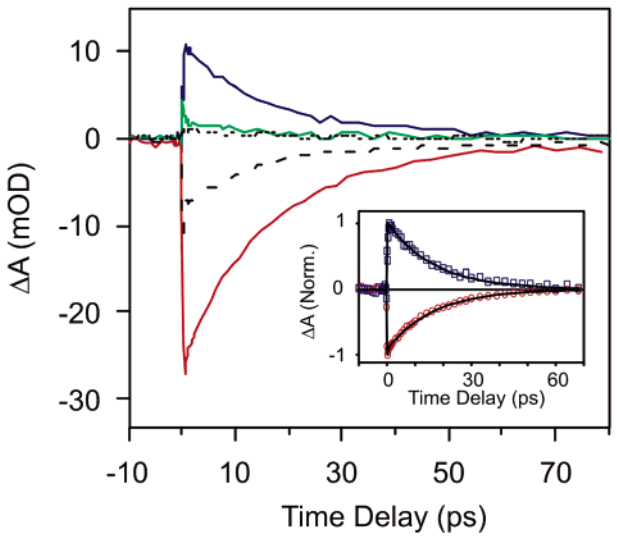

Figure 7. Transient kinetics of CNCbl in ethanol after 400 nm excitation. Probe wavelengths are top to bottom 480 (blue), 600 (green), 620 (dots), 520 (dashed), 550 nm (red). (Inset) Fit of the data obtained at 480 and 550 nm.

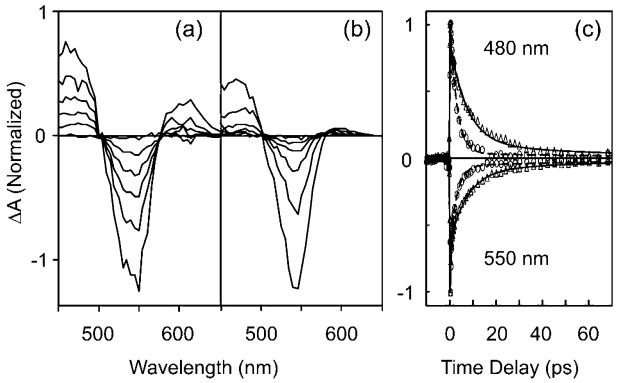

Figure 8. Transient difference spectra for (a) N_3Cbl and (b) H_2OCbl solutions in ethanol at 0.4, 2, 5, 10, 20, and 100 ps after 400 nm excitation. Spectra for N_3Cbl and H_2OCbl were scaled to have the same value at the peak of the bleach at 0.4 ps. (c) Transient kinetic traces at 480 and 550 nm for N_3Cbl (triangles) and H_2OCbl (circles) in ethanol. The lines are the fits to the data.

in Figure 5 for CNCbl in water also illustrate the dependence of the observed signal on the intensity of the pump pulse. The laser system was capable of supplying a 400-nm pump pulse with a pulse energy of ca. 25 μJ/pulse. In general a neutral density filter in the pump beam allowed the attenuation of the beam to intensities on the order on a microjoule. Attenuation of the pump is important for CNCbl and other cobalamins, as the cross section for two-photon dissociation can be substantial. The second trace, plotted in blue, exhibits the same 6.7 ps decay component found in the other scans, but also exhibits a much longer decay component, attributed to formation of a long-lived photoproduct following excitation with an intense 400 nm pulse. With the exception of this trace, all of the visible absorption data reported here were obtained with pulse energies of ca. 1−3 μJ. A somewhat higher pump power with a larger focal spot (7 μJ in 0.5 mm) was used when measuring the transient IR spectra of cyanocobalamin.

The initial evolution of the excited state was probed in a one-color experiment using the output of the NOPA at 520 nm to produce both the excitation and probe pulses. This trace is plotted in Figure 6. The cross correlation of the pump and probe pulses was determined by using an optical Kerr effect measurement in CCl_4 in a similar flow cell located at the position used for the transient absorption measurements. The cross correlation of the pulse is modeled well by a Gaussian profile with a fwhm of 40 ± 2 fs. The deconvoluted fwhm of the pulse is 28 fs.

The data obtained at 520 nm exhibit an instrument-limited appearance of the bleaching signal; an additional 80 fs increase in the bleaching signal followed by a 190 fs decay of the bleach is also observed. The overall decay of the bleaching signal to baseline occurs with the same 6.7 ps time constant observed for the other probe wavelengths. There is no evidence of a recurring oscillation in the data, and no suggestion of a substantial impulsive geometry change following excitation. The overall signal reflects rapid subpicosecond internal conversion to the lowest excited state followed by picosecond internal conversion to the ground electronic state.

The excited-state decay in ethanol is qualitatively similar, but substantially slower than that observed in water. The evolution of the difference signal for CNCbl in ethanol is shown in Figure 7 for several probe wavelengths ranging from 480 to 620 nm. For delay times >1 ps, all of the traces have the same decay rate within the accuracy of the measurement. These kinetics traces can be fit by instantaneous rise followed by a ~300 fs decay and a 16.5 ps decay at all wavelengths. Fits to the data obtained at 480 and 550 nm are shown in the inset in Figure 7. These data reinforce the conclusion that the overall signal reflects rapid subpicosecond internal conversion to the lowest excited state followed by picosecond internal conversion to the ground electronic state.

Visible Transient Absorption of Azidocobalamin, Aquocobalamin, and Hydroxocobalamin . Transient kinetics traces were also measured for N_3Cbl and H_2OCbl in ethanol. The transient difference spectra constructed from the kinetic traces are shown in Figure 8a and 8b. These spectra were scaled to have the same amplitude for the bleach at 0.4 ps. The transient difference spectra for N_3Cbl and H_2OCbl are similar to the difference spectra obtained for CNCbl, with a bleaching of the cob(III)alamin absorption band at 550 nm and absorption of

Table 1. Lifetime of the Excited State of CNCbl and N_3Cbl as a Function of Solvent

solvent[a]	ϵ[b]	η[c]	τ_2 (ps) CNCbl	τ_2 (ps) N_3Cbl
water	80.4	1.002	6.7	3.0
MeCN/H_2O	59	0.801	9.5	
H_2O/methanol	60.4	1.817	10.5	4.0
H_2O/ethanol	54.0	2.844	11.2	5.0
methanol	32.4	0.597	12.0	6.7
ethanol	25.0	1.200	16.5	7.5
2-Propanol	18.6	2.86	18.5	8.5
isobutyl alcohol	15.8	4.703	15.8	7.8

[a] Solvent mixtures were 50/50 by volume. [b] The solvent dielectric constants were obtained from ref 25. All values are at 20 °C except for isobutyl alcohol, which is at 25 °C from ref 26, and MeCN/H_2O, which is at 25 °C from ref 27. [c] The solvent shear viscosity in mPa.[26] All values are at 20 °C except for 2-propanol and isobutyl alcohol, which are at 15 °C[26] and MeCN/H_2O, which is at 25 °C from ref 27.

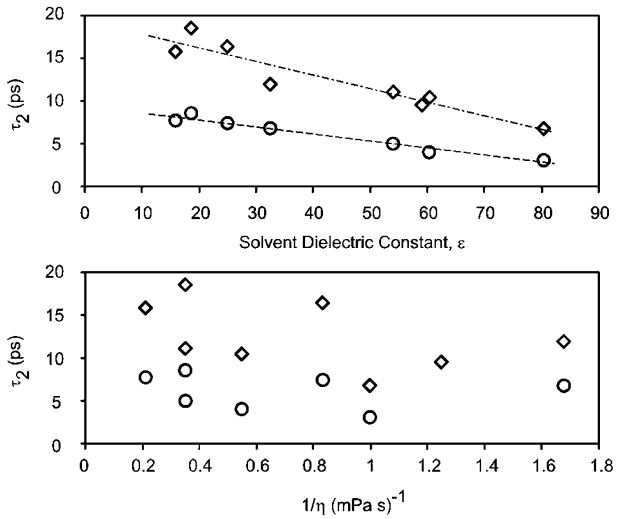

Figure 9. Excited-state lifetimes in CNCbl (diamonds) and N_3Cbl (circles) plotted as a function of the static dielectric constant of the solvent (top) and as a function of the inverse of the solvent shear viscosity (bottom).

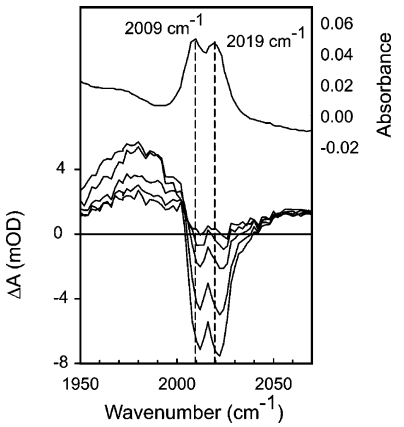

Figure 10. (a) Static FTIR and (b) transient IR difference spectra of N_3-Cbl in ethanol 2, 5, 10, 15, and 20 ps following excitation at 400 nm.

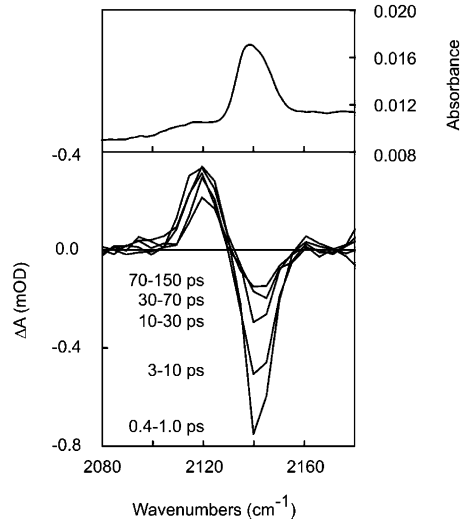

Figure 11. Static FTIR spectrum (top) and transient IR difference spectra (bottom) of CNCbl in ethanol. Each curve in the transient spectra represents an average of 5−10 spectra within the given delay time interval.

the photoproduct at both 480 and 600 nm. The decay of the signal at 480 and 500 nm is plotted in Figure 8c. The kinetics traces can be fit by an instantaneous rise followed by a ~300 fs decay and a picosecond decay to baseline at all wavelengths. The time constant for the picosecond decay is substantially faster than the decay of CNCbl. Time constants of 7.5 ps for N_3Cbl and 2.9 ps for H_2OCbl are obtained from the fit to the data. An additional long time scale, small amplitude, decay (70−100 ps) is required to fit the N_3Cbl and H_2OCbl data at some wavelengths.

Solvent Dependence of the Excited-State Lifetime. To provide more information on the nature of the excited states, we have studied the solvent dependence of excited-state lifetime. The decay of the excited state of CNCbl and N_3Cbl was measured in a range of solvents and solvent mixtures as summarized in Table 1. The excited-state lifetime of CNCbl ranges from 7 ps in water to 18 ps in 2-propanol, while the excited-state lifetime of N_3Cbl ranges from 3 ps in water to 8.5 ps in 2-propanol. For both compounds the lifetime has an inverse correlation with the solvent dielectric constant, but no correlation at all with the solvent viscosity as illustrated in Figure 9.

Infrared Transient Difference Spectroscopy. To further characterize the transient intermediate, IR difference spectra of N_3Cbl and CNCbl in ethanol solution were measured. Transient IR difference spectra obtained 2, 5, 10, 15, and 20 ps after 400 nm excitation of N_3Cbl are shown in Figure 10. The static FTIR spectrum shows a double peak at around 2009 and 2019 cm^{-1}. A single band was observed for N_3Cbl in water solution. This band can be assigned to the asymmetric stretch of N_3.[28] It is unclear why the spectrum in ethanol shows two peaks for N_3 in this region, but they may correspond to two possible orientations of the azido ligand.[29] The transient IR spectra show a bleach of the double peaks and a red-shifted positive absorption feature at about 1984 cm^{-1}. The decay of the absorption corresponds well with the recovery of the bleach. Transient IR difference spectra obtained following the 400-nm excitation of CNCbl in ethanol are shown in Figure 11. Each curve in Figure 11b represents an average of about 5−10 spectra within the given delay time interval to increase the signal-to-noise ratio of the data. A broad baseline shift due to heating of

(25) Åkerlöf, G. *J. Am. Chem. Soc.* **1932**, *54*, 4125−4139.
(26) Weast, R. C., Ed. *Handbook of Chemistry and Physics*, 62nd ed.; CRC Press: Boca Raton, FL, 1982.
(27) Cunningham, G. P.; Vidulich, G. A.; Kay, R. L. *J. Chem. Eng. Data* **1967**, *12*, 336−337.
(28) McCoy, S.; Caughey, W. S. *Biochemistry* **1970**, *9*, 2387−2393.
(29) Garau, G.; Geremia, S.; Marzilli, L. G.; Nardin, G.; Randaccio, L.; Tauzher, G. *Acta Crystallogr. B.* **2003**, *59*, 51−59.

solvent has been subtracted from the data. The bleach in the IR difference spectrum corresponds to the CN stretch band at 2138 cm^{-1} for ground-state CNCbl. The transient intermediate has a CN stretching band red-shifted by about 20 cm^{-1} from the ground state.

Discussion

The simplicity of the excited-state dynamics observed following excitation of CNCbl, N_3Cbl, and H_2OCbl is in contrast with those observed following excitation of the alkylcobalamins. In previous work we have used ultrafast spectroscopic techniques to explore the mechanism for photolysis of both of the natural coenzymes, AdoCbl and MeCbl.[7−10] In complementary studies we have also investigated the photochemistry of the synthetic alkylcobalamin analogues, ethylcobalamin (EtCbl) and *n*-propylcobalamin (PrCbl).[11] The photochemistry of the alkylcobalamins vary, but all of the compounds exhibit bond homolysis on a time scale between a few picoseconds and a few hundred picoseconds, followed by a competition between recombination and the formation of a long-lived radical pair. By contrast, the non-alkylcob(III)alamins, CNCbl, N_3Cbl, and H_2OCbl, undergo subpicosecond relaxation and internal conversion to an excited electronic state that undergoes radiationless decay to the ground state within picoseconds. The observation of clean isosbestic points in the difference spectra demonstrates that very little if any additional relaxation occurs.

Calculated Electronic Structure of Cob(III)alamins. Several time-dependent density functional (TD-DFT) calculations of the electronic structure and electronic spectrum of cobalamins have appeared in the literature recently.[15,16,18,30] Of these papers, three report calculations for CNCbl models,[15,16,18] one paper reports a calculation for the corrin ring lacking either axial ligand,[30] one paper reports calculations for cob(II)alamin,[31] one reports calculations for H_2OCbl,[16] one reports calculations for OHCbl,[20] and two report calculations on a methylcobalamin model.[16,17] Although these calculations do not yet provide a complete picture of the electronic structure of alkylcobalamins, they provide significant insight into the electronic structure of cobalamins.

The consensus of the DFT calculations for CNCbl is similar to that reported in earlier semiempirical calculations.[32−35] The lowest energy transition, corresponding to the $\alpha\beta$ band in the observed spectrum, is dominated by the HOMO → LUMO transition, predominantly a $\pi \rightarrow \pi^*$ transition of the corrin ring, polarized along the axis running between carbons 5 and 15 in Figure 1. In this transition, electron density is transferred from the axial ligands to the corrin ring. The γ band in CNCbl is polarized along the Co−C(10) axis at 90° to the polarization of the $\alpha\beta$ band while the DE-band, located between the $\alpha\beta$ and γ bands, is polarized at a small angle from the Co−C(10) axis.[16,33] The structure in the $\alpha\beta$ band, clearly seen in the spectrum of CNCbl, is generally interpreted as a vibrational progression in the lowest electronic state, although this assignment is not entirely clear.[36] It is clear that at least one additional electronic state contributes to the absorption of cobalamins in this region.[16]

The TD-DFT calculations of CNCbl reported by Stich et al.[16] and Andruniow et al.[15] are in good agreement with each other. Both of these groups have included plots of the highest occupied and lowest unoccupied MOs of CNCbl. On the basis of these molecular orbitals it is evident that the HOMO-to-LUMO transition is characterized by a reduction of electron density in the Co−L axial bonds. The HOMO exhibits a substantial contribution from electron density on the CN ligand, and in the bond between the imidazole nitrogen and the cobalt, whereas the LUMO has no significant electron density between the Co and either of the axial ligands. These calculations suggest that population of the S_1 excited state should result in a weakening of the bonds to the axial ligands and possibly cleavage of one or the other of the two bonds. On the other hand, unlike alkylcobalamins where the C−Co stretching vibration is enhanced in resonance with the α band,[16,37−40] resonance Raman measurements of CNCbl do not show an enhanced C−Co stretching vibration.[16,41,42] The vertical excitation does not involve substantial displacement or frequency change along this coordinate.

Stich el al. have also reported calculations of the electronic molecular orbitals and UV−visible absorption spectrum of H_2OCbl.[16] In contrast to CNCbl and MeCbl, the lowest electronic state of H_2OCbl is not the HOMO → LUMO $\pi\pi^*$ state, which is calculated to be S_4 at the ground-state equilibrium geometry. The lowest allowed electronic state of H_2OCbl corresponds to a weakly allowed S_3 HOMO → Co $3d_{z^2}$ LMCT state, with two, lower, forbidden states implied, but not described by Stich et al.[16] The contrast between H_2OCbl and the other two cobalamins, CNCbl and MeCbl, is a consequence of the stabilization of the Co $3d_{z^2}$ orbital in H_2OCbl. This orbital is calculated as LUMO+3 in MeCbl and LUMO+2 in CNCbl but is nearly isoenergetic with the lowest π^* orbital of the corrin ring in H_2OCbl.[16] The HOMO (corrin π) and LUMO (corrin π^*) for H_2OCbl exhibit little electron density between the Co and the axial ligands, whereas the LUMO+1 Co $3d_{z^2}$ orbital is antibonding between the Co and both axial ligands. These calculations suggest that population of the lowest excited states should result in a weakening of the bonds to the axial ligands and possibly cleavage of one or the other of the two bonds.

Nature of the Intermediate Electronic State. The transient intermediate state formed within a few hundred femtoseconds of excitation is similar in all three compounds investigated here and is formed rapidly following excitation of CNCbl at either 400 or 520 nm. In CNCbl this state is characterized by a CN stretching band at 2120 cm^{-1}, red-shifted relative to the CN

(30) Jaworska, M.; Lodowski, P. *J. Mol. Struct. (THEOCHEM)* **2003**, *631*, 209−223.
(31) Stich, T. A.; Buan, N. R.; Brunold, T. C. *J. Am. Chem. Soc.* **2004**, *126*, 9735−9749.
(32) Day, P. *Coord. Chem. Rev.* **1967**, *2*, 99−108.
(33) Fugate, R. D.; Chin, C.-A.; Song, P.-S. *Biochim. Biophys. Acta* **1976**, *421*, 1−11.
(34) Salem, L.; Eisenstein, O.; Anh, N. T.; Burgi, H. B.; Devaquet, A.; Segal, G.; Veillard, A. *Nouv. J. Chim.* **1977**, *1*, 335−348.
(35) Schrauzer, G. N.; Lee, L. P.; Sibert, J. W. *J. Am. Chem. Soc.* **1970**, *92*, 2997−3005.
(36) Sension, R. J.; Harris, D. A.; Cole, A. G. *J. Phys. Chem. B* **2005**, *109*, 21954−21962.
(37) Dong, S.; Padmakumar, R.; Banerjee, R.; Spiro, T. G. *J. Am. Chem. Soc.* **1996**, *118*, 9182−9183.
(38) Dong, S.; Padmakumar, R.; Maiti, N.; Banerjee, R.; Spiro, T. G. *J. Am. Chem. Soc.* **1998**, *120*, 9947−9948.
(39) Dong, S.; Padmakumar, R.; Banerjee, R.; Spiro, T. G. *J. Am. Chem. Soc.* **1999**, *121*, 7063−7070.
(40) Huhta, M. S.; Chen, H.-P.; Hemann, C.; Hille, C. R.; Marsh, E. N. G. *Biochem. J.* **2001**, *355*, 131−137.
(41) Mayer, E.; Gardiner, D. J.; Hester, R. E. *Biochim. Biophys. Acta* **1973**, *297*, 568−570.
(42) Mayer, E.; Gardiner, D. J.; Hester, R. E. *J. Chem. Soc., Faraday Trans. 2* **1973**, *69*, 1350−1358.

stretching frequency in the ground state. However, the frequency of the CN stretch is still significantly higher than that of CN^-, at 2080 cm^{-1},[43] or that of CN radical, observed at 2046 cm^{-1} in a matrix.[44] The frequency of the CN stretching mode in the excited electronic state indicates that the CN^- ligand is still coordinated with the Co center. A similar correspondence is also found for N_3Cbl. This conclusion is consistent with the complete recovery of the ground state within a few tens of picoseconds for all of the cobalamins studied here. Thus, the intermediate state may be attributed to a nondissociative excited state. This state is almost certainly the lowest excited singlet state of the non-alkylcob(III)alamins, although it is not necessarily the lowest vertical state at the ground-state equilibrium configuration. The finite lifetime and the lack of observable fluorescence demonstrate that the lowest excited electronic state is not the vertical HOMO → LUMO $\pi\pi^*$ excited state.

In cyanide the σ orbital originating from the lone pair electrons on the carbon atom has antibonding character toward the CN bond.[45] Bonding of CN^- with a metal tends to reduce this antibonding character and to increase the CN stretching frequency. Thus, the observed red-shift in the CN^- stretching frequency from 2138 cm^{-1} in the ground state to 2120 cm^{-1} in the excited state indicates that there is a decrease in the Co−C bond strength with a concomitant increase in antibonding character in the CN bond in the excited state relative to that in the ground state. The effect of a weakened Co−N bond on the frequency of the N_3 ligand in N_3Cbl is less well understood and will not be discussed here.[28]

The visible absorption spectrum of the excited state will also shed light on the nature of the intermediate state. This visible spectrum may be estimated from the measured difference spectrum DS(λ) and the steady-state spectrum of the cob(III)alamin SS(λ) using ES(λ) = SS(λ) + α DS(λ) where α is a variable parameter. The results of this analysis for CNCbl in water with three values of α are shown in Figure 12a. The dot−dashed line represents a lower limit for α, while the dashed line represents an upper limit. As α decreases, the predicted spectrum of the excited state approaches that of the CNCbl starting material. However, the absolute magnitude of the photoinduced bleach following excitation of CNCbl is comparable to that observed for the alkylcobalamins, setting a lower limit for reasonable values of α. An absolute upper limit for α is set by the requirement that the spectrum of the excited state be positive or zero for all wavelengths. A practical upper limit for α is set by the expectation that the spectrum will be slowly varying through the visible. The spectrum of the excited state of CNCbl in ethanol deduced from the transient difference spectrum is similar, although the red tail of the absorption spectrum is much smaller (Figure 12b).

The observed excited-state spectrum has a shape similar to that observed for species lacking an axial base (alkylcobinamides, lacking the phosphate link and the DMB base, and for alkylcobalamins at low pH where the DMB base is replaced by a water ligand). However, the peak of the excited-state spectrum is red-shifted by ca. 35 nm with respect to species lacking an axial base. Unlike the alkylcobalamins, CNCbl remains base-on in acidic solution, even at pH 1, making a direct comparison with the CNCbl base-off spectrum difficult. A spectrum of cyanocobinamide reported by Hamza and Pratt exhibits the predicted blue-shift from the CNCbl spectrum but is more structured than the excited-state spectrum reported here (see Figure 1).[13] In addition, the short-lived excited-state spectrum exhibits a pronounced red absorption tail in water, not observed in alkylcobalamins at low pH or in cobinamides. Thus, the excited state is not a simple base-off species, but the spectrum is consistent with that of a weakened or lengthened axial Co−N bond, as well as a weakened or lengthened Co−X bond to the upper axial ligand.

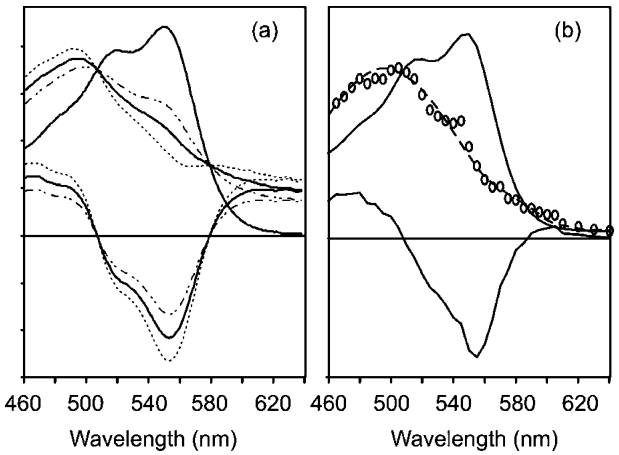

Figure 12. Estimated excited-state spectrum. The steady-state spectrum of CNCbl and the measured difference spectrum (Figure 4) are used to estimate the spectrum of the excited state from ES(λ) = SS(λ) + α DS(λ), where SS(λ) is the steady-state spectrum, DS(λ) is the measured difference spectrum and α is a variable parameter. (a) Estimated spectrum in water. The dot−dashed line represents a lower limit for α, whereas the dashed line represents an upper limit. (b) Estimated spectrum in ethanol. The excited-state spectrum is similar in both solvents, although the red edge is enhanced in water compared with that in ethanol.

Comparison with Prior Studies on Cobalt Porphyrins. Several time-resolved spectroscopic studies on related cobalt porphyrins have been reported, and these may shed some light on the nature of the intermediate electronic state formed in the cobalamin compounds studied here. In an early study of Co(II) tetraphenylporphyrin (TPP) and other Co(II) porphyrins, an excited state with <35 ps lifetime was observed and attributed to a $\pi 3d_{z^2}$ CT state.[46,47] In this study a Co(III) porphyrin, Co(III)(OEP)(CN), was also investigated. In the Co(III) porphyrin the lowest-lying excited state led to efficient CN deligation between 63 and 130 ps, and the internal conversion path was described as $\pi\pi^* \rightarrow \pi d_{z^2} \rightarrow d_\pi d_{z^2}$.[46,47] In a separate study of related Co(II) porphyrins, an excited state with a 12 ps lifetime was observed and attributed to a d−d excited-state instead of a CT state.[48] More recently the excited state of Co(II) porphyrins was reexamined with femtosecond time resolution.[49] The lowest excited state was populated in 1.8 ps and decayed with a time constant of tens of picoseconds. The solvent dependence observed in this study is consistent with formation of a CT excited state followed by nonradiative decay to the ground

(43) Penneman, R. A.; Jones, L. H. *J. Chem. Phys.* **1956**, *24*, 293−296.
(44) Milligan, D. E.; Jacox, M. E. *J. Chem. Phys.* **1967**, *47*, 278−285.
(45) Fenske, R. F.; DeKock, R. L.; Sarapu, A. C. *Inorg. Chem.* **1971**, *10*, 38−43.
(46) Tait, C. D.; Holten, D.; Gouterman, M. *Chem. Phys. Lett.* **1983**, *100*, 268−272.
(47) Tait, C. D.; Holten, D.; Gouterman, M. *J. Am. Chem. Soc.* **1984**, *106*, 6653−6659.
(48) Loppnow, G. R.; Melamed, D.; Leheny, A. R.; Hamilton, A. D.; Spiro, T. G. *J. Phys. Chem.* **1993**, *97*, 8969−8975.
(49) Yu, H. Z.; Baskin, J. S.; Steiger, B.; Wan, C. Z.; Anson, F. C.; Zewail, A. H. *Chem. Phys. Lett*. **1998**, *293*, 1−8.

state.[49] Finally, a femtosecond study of TPPCo(II)NO demonstrated the dissociation of the NO ligand with unit quantum yield following excitation at 390 nm.[50,51] This result was attributed to rapid internal conversion from the initially excited $\pi\pi^*$ state of the porphyrin to a low-lying, directly dissociative, $\pi 3d_{z^2}$CT state. In all of these studies the lack of luminescence by Co(II) and Co(III) porphyrins is attributed to rapid relaxation to a low-lying $\pi 3d_{z^2}$ or d−d state. These results are consistent with the observations on cob(III)alamins reported here.

Solvent Dependence of the Excited-State Lifetime. The lack of any discernible viscosity dependence on the rate of decay of the excited state and the lack of a component corresponding to vibrational relaxation in the transient absorption signal of cob(III)alamins suggests that the geometries of the ground and excited states are similar, with the exception of the Co-L bond(s). On the other hand, the polarity dependence of the excited-state lifetime points to an excited state with an increased dipole moment relative to the ground electronic state. As solvent polarity increases, the energy difference between the lowest excited state and the ground state decreases. If the excited state is a formal charge transfer state, the decay of this CT excited state may be considered an intramolecular electron-transfer process modeled by Marcus electron transfer theory.[52] The back electron transfer would be in the Marcus inverted region. In this regime a decrease in excited-state lifetime with increasing solvent polarity is predicted, and the back electron transfer should be unaffected by solvent viscosity.[53] However, the radiationless decay from the intermediate state to the ground state need not involve a formal electron transfer in the sense of a traditional electron donor−acceptor system, and the reaction coordinate need not be solvent reorganization. Similar behavior will be expected as the energy gap decreases if the reaction coordinate involves vibrational modes of the molecule, such as the Co−L stretching vibrations. These observations are consistent with a LMCT (π3d) assignment for the intermediate state.

The Influence of the Ligand on the Excited-State Lifetime. The excited state lifetime of the non-alkylcob(III)alamin compounds investigated here depends strongly on the nature of the upper ligand, 16.5 ps for CNCbl, 7.5 ps for N_3Cbl, and 2.9 ps for H_2OCbl in ethanol. When the σ-bond donating ability of the axial ligand is larger (smaller electronegativity), a stronger σ bond is formed, and the splitting of the bonding (ligand σ orbital) and antibonding (Co $3d_{z^2}$) orbitals increases. This trend is seen in the DFT calculations on H_2OCbl and CNCbl, where the degree of σ-donating ability of the axial ligand correlates with the destabilization of Co 3d orbitals.[16] The σ-donating ability of ligands is also correlated with the position of the γ band of cobalamins. Stronger σ-donating ligands result in a larger red-shift of this absorption band. According to previous studies, the σ-donating ability of the three ligands decreases as follows: CN > N_3 > H_2O.[5,24] As a result, the energy gap between the relaxed lowest energy excited state and the ground state should decrease in the same order. The observed lifetimes of the excited state, with τ_2(CN) > τ_2(N_3) > τ_2(H_2O), are thus consistent with the trend of decreasing driving force. The variation in rate with axial ligand provides support for the assignment of the observed excited electronic state to the $\pi 3d_{z^2}$ LMCT state.

Relationship to Excited Electronic States in Alkylcobalamins. The lowest excited state observed following excitation of the cob(III)alamins studied here has spectral characteristics distinct from the intermediate states observed following excitation of alkylcobalamins. All of the alkylcobalamins studied to date, MeCbl, AdoCbl, EtCbl (ethylcobalamin), and PrCbl (*n*-propylcobalamin), undergo bond homolysis following excitation at 400 or 520 nm. However a distinct intermediate electronic state is observed for the following: MeCbl in water, in ethylene glycol, or bound to methionine synthase;[7,9,36] EtCbl and PrCbl excited at 520 nm in water;[11] and AdoCbl when bound to glutamate mutase.[12,54] This intermediate state has an electronic absorption spectrum characteristic of that of cob(III)alamin with a σ-donating alkyl anion ligand, rather than a Co−C covalent bond.[7] The intermediate state observed in alkylcobalamins is better characterized as a metal-to-ligand charge transfer (MLCT) state, Co → R, in contrast to the LMCT excited state (corrin π → Co) observed following excitation of the typical cob(III)alamins investigated here.

On the other hand, a significant difference between the molecular orbitals calculated for MeCbl, and those calculated for H_2OCbl and CNCbl is a substantial mixing of the Me $2p_z$ and Co $3d_{z^2}$ orbitals.[16] Thus, the so-called Co $3d_{z^2}$ orbital at the vertical geometry is characterized in these three models as 62% Co, 6% H_2O; 57% Co, 11% CN; and 49% Co, 22% Me.[16] This trend, carried through to the relaxed geometry may account for the differences in the spectrum of the low-lying excited electronic state in alkylcobalamins and typical cob(III)alamin.

Summary and Conclusions

Transient absorption measurements of CNCbl, N_3Cbl, and H_2OCbl demonstrate that the photostability of Vitamin B_{12} and other cob(III)alamins arises from fast internal conversion and radiationless decay to the ground state. The transient absorption spectra of CNCbl are characterized by ultrafast formation of a short-lived excited state and return to the ground state with a time constant of 6.7 ps in water and 16.5 ps in ethanol. The ultrashort excited-state lifetime in CNCbl and other non-alkylcob(III)alamins is in contrast to that in the alkylcobalamins, where excitation results in formation of a variety of intermediate states enroute to homolysis of the Co−C bond on picosecond-to-nanosecond time scales, depending on the alkyl ligand and the solvent environment. The excited state formed following excitation of CNCbl has a distinctive absorption spectrum, with features reminiscent of species lacking an axial base such as cobinamides or base-off cobalamins. This observation is consistent with a weakening of both the axial Co−N and Co−X bonds in the excited state. The lowest excited state of the non-alkylcob(III)alamins is assigned to a $\pi 3d_{z^2}$ LMCT state on the basis of the features of the IR and visible absorption spectra of this state and on the dependence of lifetime on the solvent polarity and σ-donating strength of the axial ligand.

Acknowledgment. This work was supported by Grants NSF CHE 0078972, and NIH DK53842 to R.J.S.; NSF CHE-0135427 to T.L.; and by NIH Grant GM29225 to L.G.M.

JA054374+

(50) Morlino, E. A.; Walker, L. A., II; Sension, R. J.; Rodgers, M. A. J. *J. Am. Chem. Soc.* **1995**, *117*, 4429−4430.
(51) Morlino, E. A.; Rodgers, M. A. J. *J. Am. Chem. Soc.* **1996**, *118*, 11798−11804.
(52) Marcus, R. A. *Angew. Chem., Int. Ed. Engl.* **1993**, *32*, 1111−1121.
(53) Cukier, R. I.; Nocera, D. G. *J. Chem. Phys.* **1992**, *97*, 7371−7376.
(54) Sension, R. J.; Harris, D. A.; Stickrath, A.; Cole, A. G.; Fox, C. C.; Marsh, E. N. G. *J. Phys. Chem. B* **2005**, *109*, 18146−18152.